Scientia Africana, Vol. 10 (No.1), June 2011, pp

SIMULATION OF DIRECT-SEQUENCE ULTRA-WIDEBAND USING SIMULINK

O. Anyaegbu, J. N. Dike and A. A. Eteng
Department of Electrical/Electronic Engineering
University of Port-Harcourt,
Port-Harcourt, Nigeria

ABSTRACT
Owing to the increasing use of Wireless Personal Area Networks (WPANs) in which users can connect devices such as mobile phones, printers and computers without using physical cables over short-range wireless links, the need for improved channel capacity has become an issue. Direct-sequence ultra-wideband (UWB) is an impulse-based scheme that provides a direct means of increasing transmission bandwidth, thereby enabling data to be transmitted at very high bit rates. This paper describes the simulation of a single-user end-to-end direct-sequence UWB link in an Additive White Gaussian Noise (AWGN) channel using SIMULINK. The simulated bit error-rate characteristics indicate that reliable high bit-rate communication can be achieved in the presence of AWGN using direct-sequence UWB.

Keywords: Direct-sequence, Ultra-wideband, Narrowband, bandwidth, simulation, wireless

INTRODUCTION

Narrowband radio has over time been the traditional means of wireless communication. However, in the strictest sense, no wireless communication is band-limited. Rather, beyond the spectral boundaries apportioned to a system, there is some amount of incidental radiated power, making it necessary for the definition of power limits for these out-of-band radiations (Eteng, 2008).

The inherent narrowband nature of earlier wireless communication technologies such as Wi-Fi (IEEE 802.11) and Bluetooth limits their achievable data capacity. However, the enormous bandwidth of ultra-wideband signals, theoretically should give Ultra-wideband (UWB) technology an edge over the narrowband technologies. In addition, the spectral power density of UWB signals should, in principle, allow them to coexist with other existing systems. These two major attractions have provided the motivation for the development of high-data rate WPANs based on UWB technology.

Historically, the origins of UWB as a communication scheme can be traced to the late 1990s, when in a bid to obtain more channel capacity from the tightly regulated frequency spectrum some companies in the U.S. began to argue for intentional transmission at those incidental power limits. Such transmissions were to be based on the use of UWB signals. UWB signals can be described as those signals with a fractional bandwidth greater than 0.20. Fractional bandwidth, on the other hand, is defined by the following equation:

$$B_f = \frac{B}{F_c} = 2\frac{F_h - F_l}{F_h + F_l} \quad \ldots\ldots\ldots(1)$$

Where:

B_f is the fractional bandwidth,
B is the actual bandwidth,
F_c represents the carrier frequency,
F_h is the upper cut-off frequency,
F_l is the lower cut-off frequency.

An alternate definition classifies UWB signals as those signals with an ‘ultra-wide bandwidth’ greater than 500MHz. Ultra-wide bandwidth, in this case, is defined as, “the frequency band bounded by the points that are 10dB below the

Scientia Africana, Vol. 10 (No.1), June 2011. pp 41-45
 ISSN 1118 - 1931

highest radiated emission" (Federal Communications Commission, 2002).

Shannon's channel capacity theorem clearly shows the reasons for advocating an increased bandwidth (McCorkle, 2002). By the theorem, channel capacity is given by:

$$C = B\log\left(1+\frac{S}{N}\right) \quad \text{……… (2)}$$

Where:

C is channel capacity,

B represents signal bandwidth

S stands for signal power,

N represents the noise power.

This theorem reveals that narrowband systems have to strike a balance between increased channel capacities and transmit power. If the bandwidth is constrained, the required transmit power increases exponentially with increase in the channel capacity or data rate. However, channel capacity scales linearly with bandwidth. Consequently, UWB signals have the potential of achieving very high data rates with relatively low transmit power.

Broadly speaking, there are two classes of UWB radio systems, namely:

1. Multiband UWB, in which the UWB spectrum is split into sub-bands;
2. Impulse radio, in which the full UWB spectrum is utilized by generating very short duty-cycle pulses in the time-domain.

Direct-sequence UWB is an impulse radio scheme implemented using time-domain signal processing for the transmission and reception of information. This work demonstrates a simulation of this UWB scheme in an Additive White Gaussian Noise (AWGN) channel.

THE DIRECT-SEQUENCE UWB TECHNIQUE

Information to be transmitted using direct-sequence UWB must first be in digital format. In other words, the information to be transmitted must be a bit sequence. Before these information symbols are transmitted, they are first multiplied by a pseudorandom binary-valued chip sequence. Chips are bits of shorter duration than the information bits. This action results in the spreading of the bandwidth of the digital information sequence. This 'spread' sequence can now serve as input to a signal generator that will generate the appropriate UWB pulse for transmission. It should be noted, however, that if this sequence were transmitted just as developed, synchronization between the transmitter and receiver will very likely be lost when there is a transmission of a long sequence of ones or zeros. To combat this, the 'spread' sequence must be digitally phase-modulated using binary phase shift keying (BPSK).

At the receiver, the received sequence of information symbols has to be de-spread by multiplying it with the same pseudorandom sequence used for spreading at the transmitter end. The use of different pseudorandom sequences for different users lends multiple access capabilities to the direct-sequence UWB system.

Although any pulse shape may be used for UWB communications, the most commonly used pulse shape in the analysis of UWB systems is the Gaussian pulse. This preference is due to the mathematical tractability and ease of generation of this pulse shape (Miller, 2003). Analytically, it is described by:

$$x(t) = Ae^{-\frac{(t-\mu)^2}{2\sigma^2}} \quad \text{……….(3)}$$

Where:

A is the pulse amplitude in volts,

t is the time in seconds,

σ is the standard deviation of the Gaussian pulse in seconds,

μ is the mean value of the Gaussian pulse in seconds,

$x(t)$ is the pulse at time t.

Scientia Africana, Vol. 10 (No.1), June 2011. pp 46-57
© Faculty of Science, University of Port Harcourt. Printed in Nigeria. *ISSN 1118 - 1931*

The duration of the Gaussian pulse τ in seconds is given by:

$\tau = 2\pi\sigma$ ……………..(4)

For UWB schemes, τ is typically in the order of one nanosecond or less.

The typical Gaussian pulse has d.c. spectral components. Antennas, however, are unable to radiate d.c. components. Therefore, the use of the Gaussian pulse for information transmission will result in signal distortion at the transmitting and receiving antennas. Consequently, higher-order derivatives of the Gaussian pulse, which do not contain d.c. components are employed for characterizations of UWB communications. These derivatives can be recursively obtained from the relation:

$$x^{(n)}(t) = -\frac{n-1}{\sigma^2} x^{(n-2)}(t) - \frac{t}{\sigma^2} x^{(n-1)},$$

……..(5)

where n is the order of the derivative. (Wessman et al, 2005).

SIMULATION METHODOLOGY

The simulation software employed in this study is SIMULINK 7.0 running within MATLAB version 7.5 (R2007b). The simulation is logically divided into three stages, namely:

1. signal generation
2. channel modeling
3. signal reception

Signal Generation

The following parameters are used in simulating the generation of direct-sequence UWB pulses:

a) The UWB pulse is a fourth-order derivative Gaussian pulse with duration of 0.5ns.

b) Chip duration is 0.5ns.

c) Pseudorandom code type is the gold code.

d) Length of chip sequence is 39 chips.

e) The data rate is

$$\frac{1}{0.5 \times 10^{-9} \times 39} = 51.3Mbps$$

The process by which the direct-sequence UWB pulses are generated is highlighted in the following steps:

1. Arbitrary data bits representing the digitized information to be transmitted are first generated. Mathematically, this stream of data bits *s(t)* can be represented as:

$$s(t) = \sum_j b_j(T_b)$$ ………………(6)

b_j represents the *j-th* data bit, while T_b is the duration of this bit. To implement this step in SIMULINK, a sub-system block, 'User Data', is created as shown in Figure 1.

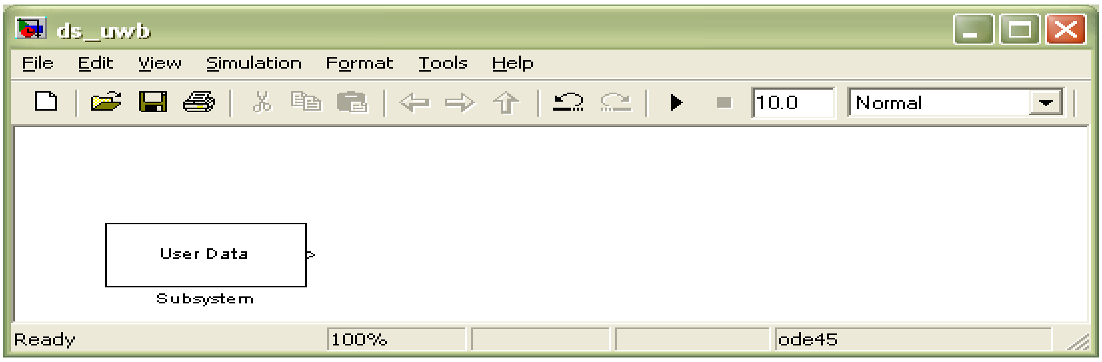

Figure 1: 'User Data' sub-system block

Scientia Africana, Vol. 10 (No.1), June 2011. pp 41-45
© Faculty of Science, University of Port Harcourt. Printed in Nigeria. *ISSN 1118 - 1931*

This block contains a binary sequence generator that generates a Bernoulli distributed sequence of bits, as shown in Figure 2.

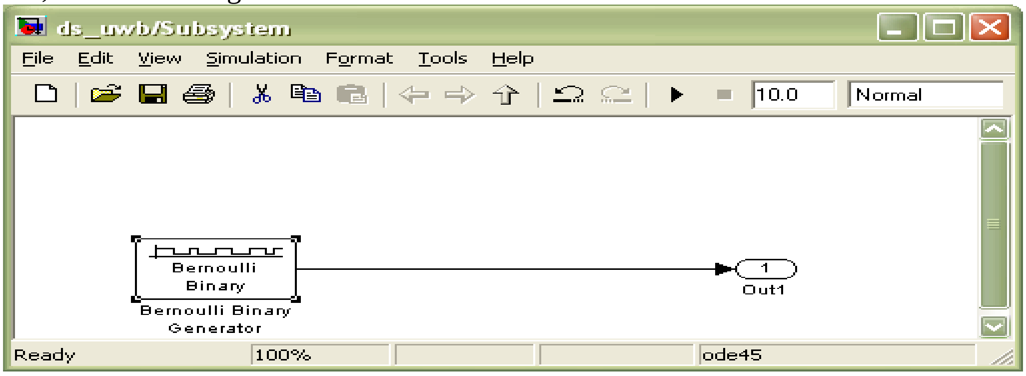

Figure 2: Contents of 'User Data' sub-system block

2. Next, the generated data bits are multiplied by a pseudorandom code sequence, with each bit multiplied by a time-coincident group of shorter duration chips. The result of this operation is that the data bits are spread over a larger number of chips. Mathematically, this operation is represented as:

$$s(t) = \sum_{j}\left[b_j(T_b) \times \sum_{n}^{N_{b-1}} c_n(T_c) \right]$$

$$\therefore s(t) = \sum_{j}\sum_{n}^{N_{b-1}} c_n b_j (jT_b + nT_c) \quad \ldots\ldots\ldots (8)$$

c_n and T_c represent the spreading chips, and their durations respectively. Each bit b_j is multiplied by $N_{b-1} - n$ chips time-coincident chips.

This step is implemented in SIMULINK by first creating a 'Code Generator' sub-system block, which contains a Gold sequence generator, as shown in Figure 3. The length of the code is equal to $N_{b-1} - n$, which in this simulation is chosen to be 39. T_c is chosen as 0.5 ns.

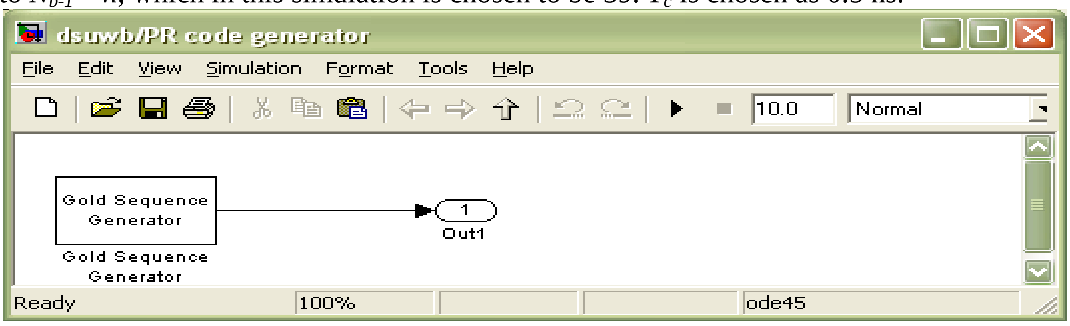

Figure 3: The Code Generator sub-system

The output of the 'Code Generator' block consists of chips, which are then multiplied with the sequence of data bits in a 'Data Spreader' block, as shown in Figure 4.

Scientia Africana, Vol. 10 (No.1), June 2011. pp 46-57
© Faculty of Science, University of Port Harcourt. Printed in Nigeria. *ISSN 1118 - 1931*

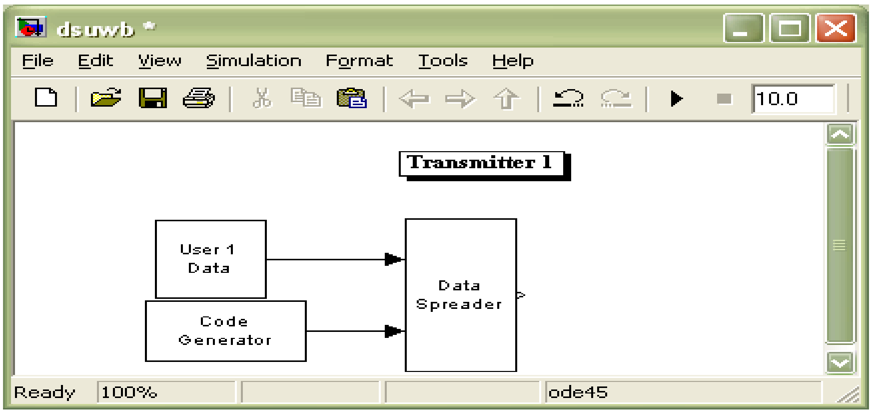

Figure 4: Spreading of data bits by generated chips

3. The spread sequence of data bits is then modulated using binary phase shift keying (BPSK). Mathematically, this represented as:

$$s(t) = \sum_{j} \sum_{n}^{N_{b-1}} c_n b_j (t - jT_b - nT_c) \qquad \text{.....................................equation 9}$$

This step can be implemented in SIMULINK by creating a 'Real BPSK Modulator' sub-system, comprising of a BPSK modulator and a complex-to-real converter block 'Re(u)' to extract the real part of the resulting complex signal. This is informed by the fact that the imaginary part of the signal doesn't contribute to the physical signal to be generated, but exists for a complete mathematical representation of the signal. Figure 5 is an illustration of this step.

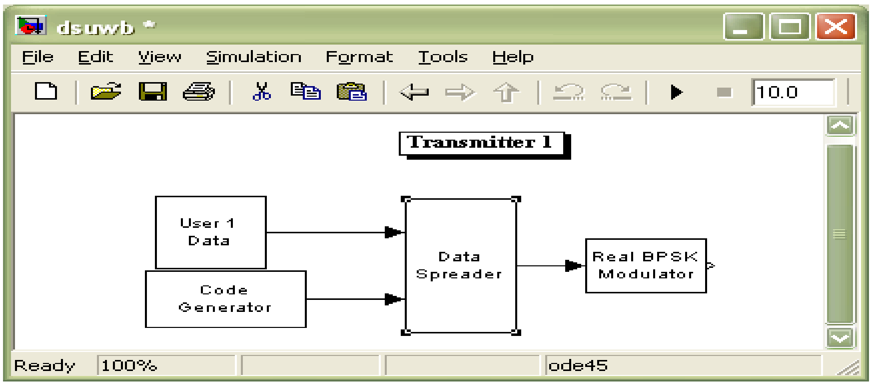

Figure 5: BPSK modulation

4. The output of the modulation stage serves as input to a pulse-shaping filter, which provides the required fourth-order derivative Gaussian pulses. This operation results in a data stream that can be represented thus:

$$s(t) = \sum_{j} \sum_{n}^{N_{b-1}} c_n b_j x(t - jT_b - nT_c) \qquad (10)$$

$x(t - jT_b - nT_c)$ represents BPSK modulated spread data bits, shaped in the form of fourth-order derivative Gaussian pulses. At this point, $s(t)$ is a stream of direct-sequence UWB pulses.

Scientia Africana, Vol. 10 (No.1), June 2011. pp 41-45
© Faculty of Science, University of Port Harcourt. Printed in Nigeria. *ISSN 1118 - 1931*

To simulate this step, a 'Pulse Shaping Filter' block is created, into which the modulated sequence is sent, as shown in Figure 6.

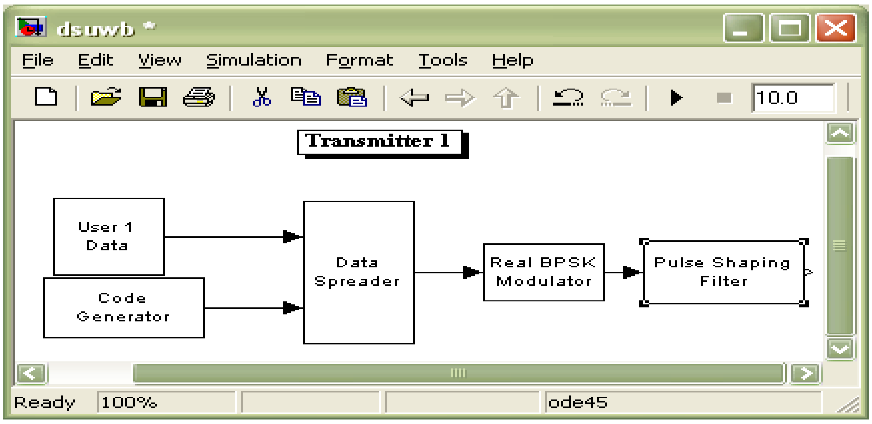

Figure 6: Passing the modulated bit sequence to the Pulse Shaping Filter

Internally, the 'Pulse Shaping Filter' subsystem block consists of an 'Unbuffer' block and an S-Function block, as shown in Figure 7 below.

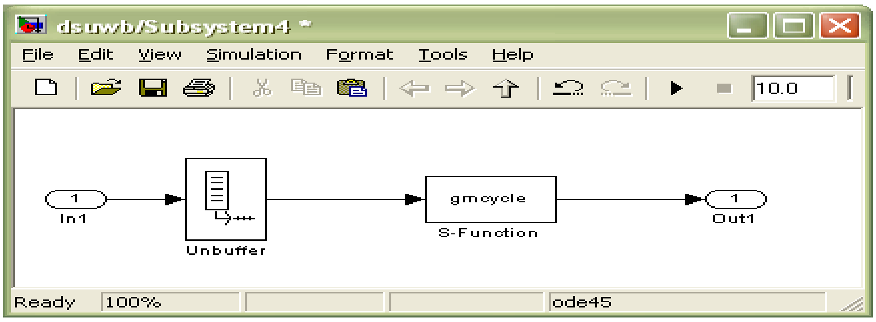

Figure 7: Contents of the 'Pulse Shaping Filter'

The S-Function block implements an S-Function, 'gmcycle', written in MATLAB to implement the generation of fourth-order derivative Gaussian pulses. The 'Unbuffer' block is used to change the format of the incoming bit sequence to a form that can serve as input to the S-Function.

Channel Modeling

The channel model adopted in this simulation is the Additive White Gaussian Noise (AWGN) channel. In this channel model, an additive Gaussian distributed random noise process corrupts the transmitted signals. Physically, this noise process can arise from electronic components in a system, or from external interference usually encountered in transmission. This noise characterization spreads over the entire spectrum. The signal at the receiver front-end, $s_c(t)$, therefore, is a linear sum of transmitted signals, $s(t)$ and the channel noise $n(t)$. Concisely:

$$s_c(t) = s(t) + n(t) \quad \ldots\ldots\ldots\ldots\ldots(11)$$

In the simulation, an AWGN block is used as the channel implementation. The input to this block is the generated stream of direct-sequence UWB pulses. This is shown in Figure 8.

Scientia Africana, Vol. 10 (No.1), June 2011. pp 46-57
© Faculty of Science, University of Port Harcourt. Printed in Nigeria. ISSN 1118 - 1931

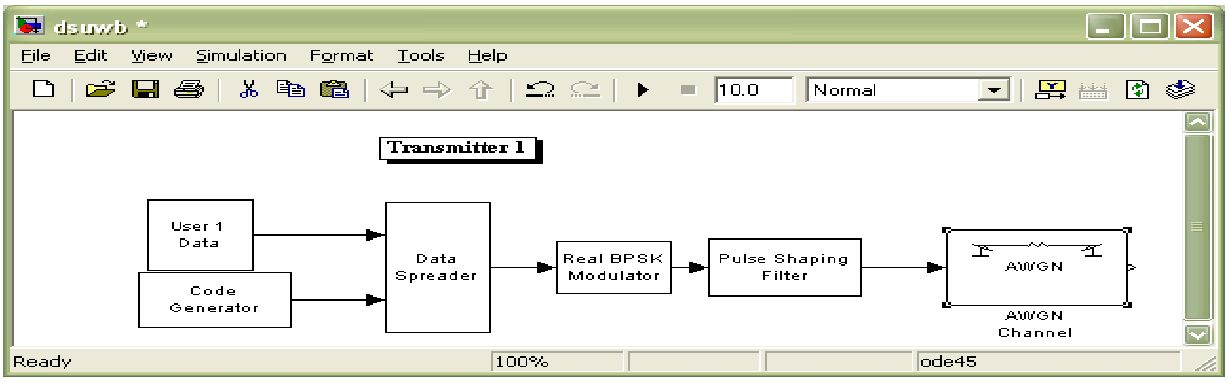

Figure 8: Adding the AWGN channel

Signal Reception

For the detection of the noise-corrupted signal, a correlator receiver is modeled. The following steps highlight the process:

1. The channel output $s_r(t)$ is correlated with a template signal *y(t)*. This template signal is identical to the generated direct-sequence UWB pulse stream, and locally synchronized to it. That is:

$$y(t) = \sum_j x(t - jT_b - nT_c) \quad \ldots\ldots(12)$$

The result of the correlation process, $s_{cor}(t)$ is:

$$s_{cor}(t) = y(t) \times [s(t) + n(t)]$$

The simulation of this step is illustrated in Figure 10.

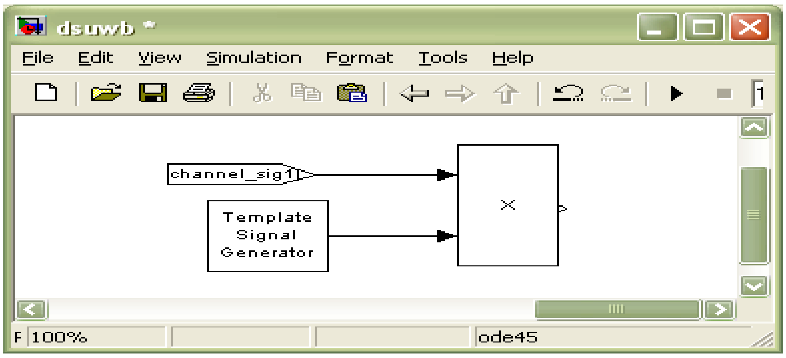

Figure 10: Correlation of channel output by template signal

Here, the output of a 'Template Signal Generator' is used to correlate the channel output. The template signal generator consists of a signal generator driven by a locally generated replica of the spreading chip code. The Signal Generator block here contains the same elements as are in the 'Pulse Shaping Filter' block shown in Figure 7. Hence, its output is also a stream of fourth-order derivative Gaussian pulses.

Scientia Africana, Vol. 10 (No.1), June 2011. pp 41-45
© Faculty of Science, University of Port Harcourt. Printed in Nigeria. *ISSN 1118 - 1931*

2. The correlated signal is integrated over a bit period (that is, the time for the occurrence of 39 chips). Mathematically,

$$s^{|}(t) = \int_{T_b} s_{corr}(t)dt \quad \ldots\ldots\ldots(13)$$

This is implemented by adding an 'Integrator' block, as shown in Figure 11. The 'Integrator' block consists of a complex-to-real converter block 'Re(u)', which extracts the real part of the now complex correlator output; an 'Integrate and Dump' block, in which the signal is integrated over successive one-bit periods; and a 'Zero-order hold'. The 'Zero-order hold' delays the result by one sample period in order to facilitate error-rate calculation later in the simulation.

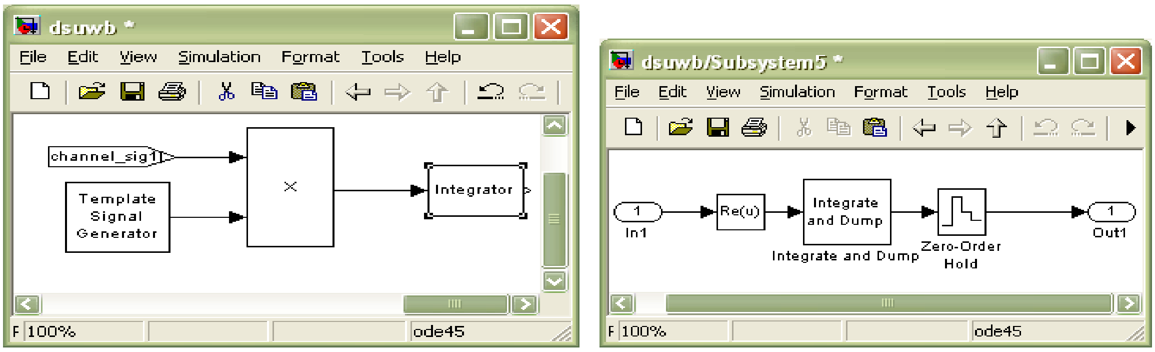

(a) Addition of the 'Integrator' block **(b) Contents of the 'Integrator' block**

Figure 11: Integration of the correlated signal

3. After the integration stage, a decision is made on whether the result represents a '0' bit or a '1' bit. This decision is reached by comparing the energy of $s^{|}(t)$ over a bit period with a threshold value. Logically,

$$s_r(t) = \begin{cases} 0, & \int_{T_b} s^{|}(t) < 0 \\ 1, & \int_{T_b} s^{|}(t) \geq 0 \end{cases}$$

The simulation of this stage is implemented by creating an S-Function block 'Decision Logic', which implements an S-Function 'threshold1' written to implement the threshold logic, as shown in Figure 12.

Scientia Africana, Vol. 10 (No.1), June 2011. pp 46-57
© Faculty of Science, University of Port Harcourt. Printed in Nigeria. *ISSN 1118 - 1931*

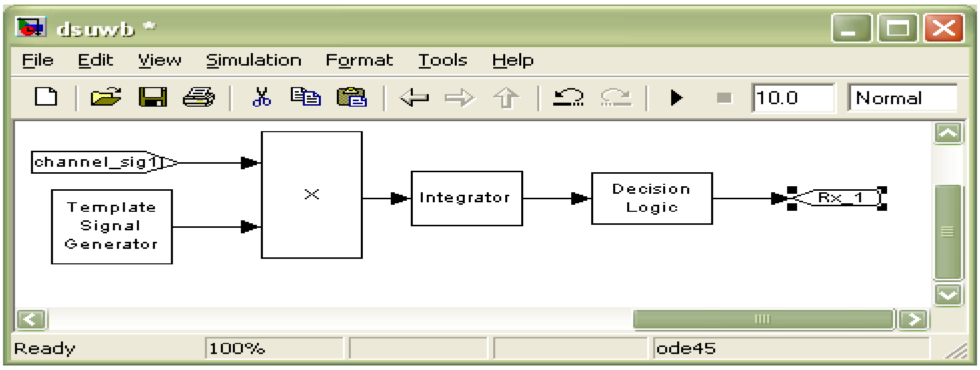

Figure 12: Addition of the threshold logic stage

The complete simulation model is shown in Figure 13. The various signals created in the simulation process can be viewed by attaching a 'Go-To' tag to the line carrying the signal of interest. A corresponding 'From' tag can then be attached to an appropriate scope to display the signal. The random data bits are compared with the receiver bit decisions, and the bit-error ratio computed.

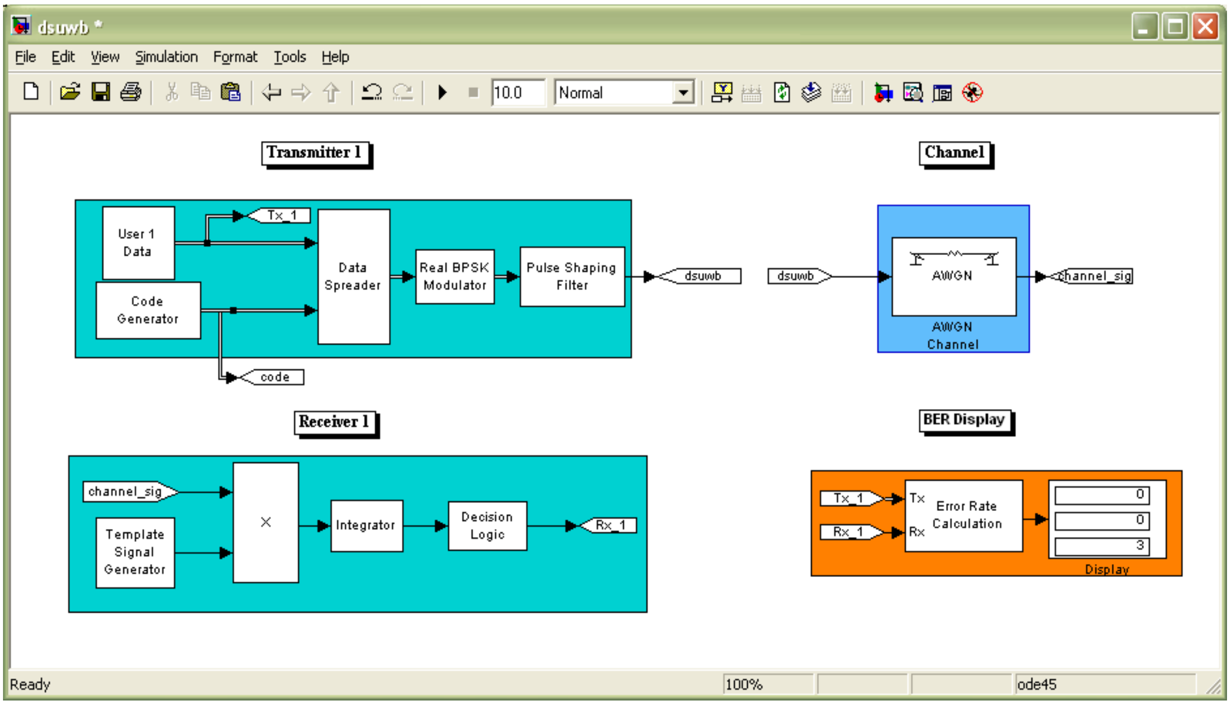

Figure 13: Complete Simulation model

DISCUSSION OF RESULTS

The simulation model was tested by transmitting a sequence of 200 data bits through the AWGN channel, while the channel signal-to-noise (SNR) was reduced from 1dB to -10dB. Figure 14 is a scope snapshot of four UWB pulses at the transmitter output, representing the 'spread' sequence '1110'. From the figure, it can be observed that each pulse lasts for 0.5ns.

Scientia Africana, Vol. 10 (No.1), June 2011. pp 41-45

ISSN 1118 - 1931

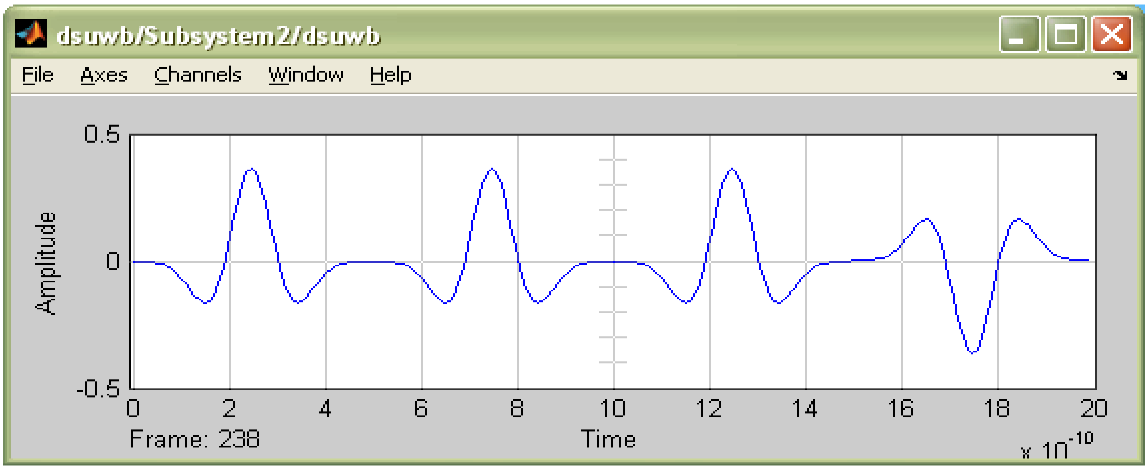

Figure 14: A vector scope display showing four UWB pulses

Figure 15 is a scope display of this same bit sequence at the output of the channel for an SNR of -2dB. From this figure it can be observed that the amplitude and phase relationships of the transmitted UWB pulses are completely lost as a result of the additive noise process. Furthermore, the amplitude range of the transmitted sequence has increased.

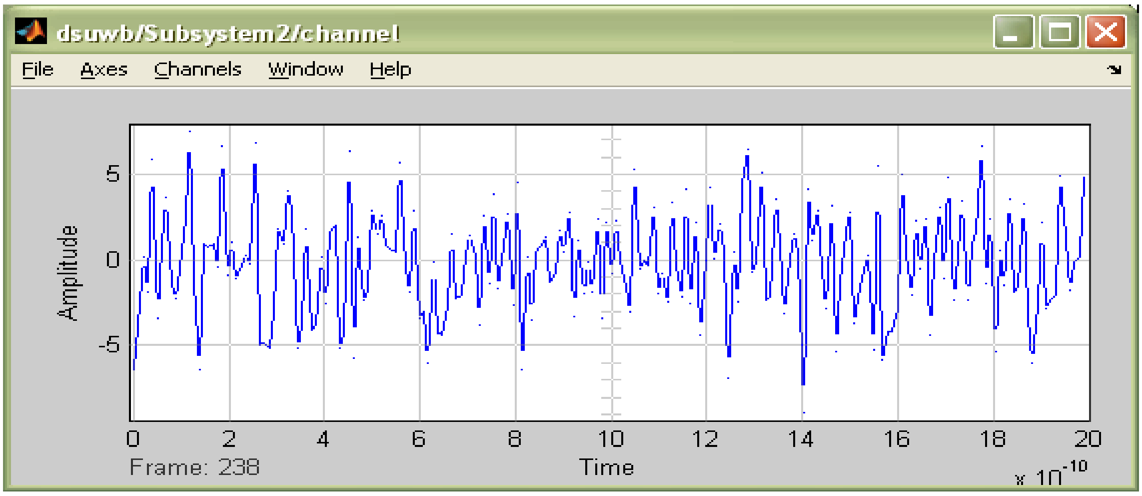

Figure 15: A vector scope display of the channel output

The receiver algorithm earlier discussed specifies that the channel corrupted signal can be recovered by implementing an integration operation after correlating the signal with a local replica of the chip sequence. Figure 16 is a scope display of the output of the integration stage.

Scientia Africana, Vol. 10 (No.1), June 2011. pp 46-57
© Faculty of Science, University of Port Harcourt. Printed in Nigeria. *ISSN 1118 - 1931*

Figure 16: Vector scope display of the output of the 'Integrator'

It can be observed from this figure that the integration operation attempts to cluster the noisy signal amplitudes into specific time slots. This is directly attributable to the 'integrate and dump' component shown in Figure 11b, and is critical for the correct reception of the original data sequence. From the receiver algorithm previously discussed, it is clear that this timing must be prearranged, as it is not extracted from the channel-corrupted signal. The hardware implementation of this step therefore demands extremely high precision timing.

It can also be observed that the maximum amplitude excursion of these 'clusters' at output of the integrator is several orders of magnitude less than the amplitude of the noisy channel output. This behaviour is typical of integrate and dump filters (Sharma, 2008). Bit decisions are reached by comparing the signal energy in these signal 'clusters' against a threshold. The implication is that the signal energy gathering implementation must be sensitive to minute amplitude changes.

To evaluate the direct-sequence UWB scheme, 11 simulations were run to obtain corresponding bit-error ratios (BER) for values of channel signal-to-noise ratio (SNR) ranging from 2dB to -10dB. The results are plotted in Figure 17.

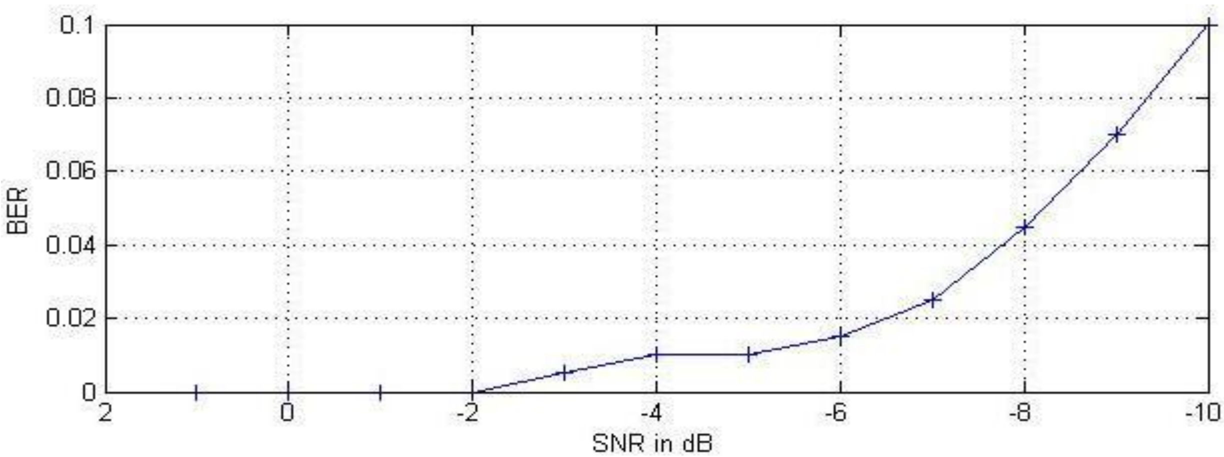

Figure 17: Plot of channel SNR against BER

Scientia Africana, Vol. 10 (No.1), June 2011. pp 41-45
© Faculty of Science, University of Port Harcourt. Printed in Nigeria. *ISSN 1118 - 1931*

From the figure it can be observed that the direct-sequence UWB scheme demonstrates high robustness against AWGN. As shown in the plot, an error rate of 10% can still be achieved without the use of error correction codes in the presence of AWGN 10dB greater than the signal power.

CONCLUSION

This simulation of direct-sequence UWB has been developed for a single-user scenario, devoid of multipath fading channel constraints. Its focus has been on the performance of the scheme in the presence of additive interference in the form of AWGN, which could typically result from thermal agitation at the front-end of radio receivers. The simulation model has been developed in SIMULINK by direct translation of mathematical models for the transmission and reception of direct-sequence UWB.

The BER results obtained show a bit-error rate of less than 10% for SNR above -10dB. These results suggest that AWGN is not a significant channel impairment to direct-sequence UWB communication links. Reliable high bit-rate direct-sequence UWB data transmissions are therefore possible in the presence of AWGN.

REFERENCES

Eteng, A. (2008): "A Comparative Analysis of Time-Modulated And Direct-Sequence Ultra-Wideband For WPANs", M.Eng Thesis: University of Port-Harcourt

Federal Communications Commission (2002): "Channel Modeling Sub-committee Report (Final)", [Online] 14 Feb., p.12. Available at:http://www.sara-group.org/official_information/specific_decisions_for_different_countries [Accessed 3 February 2010].

McCorkle, J. (2002): "Why such uproar about UWB", [internet] CommsDesign, Available at: http://www.commsdesign.com/design_corner/OEG20020301S0021____[Accessed 3 February 2010].

Miller, L. E. (2003): "Models of UWB Pulses", Draft. Wireless Communication Technologies Group, NIST, Gaithersburg Maryland. [online] Available at: http://www.antd.nist.gov/wctgmanet/Models_UWB_Pulses.pdf [Accessed 3 February 2010].

Sharma, S. (2008): Signal Theory and Processing, 6th edition, Kataria & Sons, New Dehli, p.803.

Wessman, M. & Svensson, A. (2005): "Performance of Coherent Impulse Radio and Multiband-OFDM on IEEE UWB Channels", Available at: http://document.chalmers.se/download?docid=1185604438 [Accessed 3 February 2010].